1985 ASME Presentation

THE COMPARATIVE DYNAMIC RESPONSE OF TYPICAL CLASS II PIPING WITH DIFFERENT SUPPORT CONDITIONS

by

R.S. Keowen, P. Ibanez, B.A. Johnson, and K.L. Merz
ANCO Engineers, Inc., Culver City, California

ABSTRACT

A pressurized sixty-foot section of 8-inch and 6-inch Class II piping with multiple elbows and a simulated motor-operated valve was supported on a system of shake tables and subjected to simulated earthquake input motion. Sixty-four channels of acceleration, displacement, and strain data were collected and analyzed to determine the changes in acceleration and displacement response and the changes in peak moments and ASME-allowable stresses at critical locations with three different pipe restraint devices installed at two locations on the piping system. These restraint devices, installed horizontally, consisted of rigid elements, mechanical piping snubbers, and visco-elastic piping dampers. Differences in modal dampings, modal responses, computed peak moments, and computed peak allowable stress ratios were noted for the various restraint devices.

DESCRIPTION OF THE TEST PIPING, RESTRAINT DEVICES, INPUT WAVEFORM, INSTRUMENTATION, AND DATA ACQUISITION AND ANALYSIS METHODS

The test piping system consisted of approximately sixty feet of welded 8-inch and 6-inch A-106, Grade B, Schedule 40 piping. Ten elbows and a simulated motor-operated valve were present, as pictured in Figure 1. This "typical" large-bore piping system was designed and constructed to Class II specifications. Piping size and geometry were governed by convenience of installation at the test facility and the desire to achieve several times the ASME-allowable stress limits (Ref. 1) at critical locations on the piping system within the force limits of the servo-hydraulic excitation system.

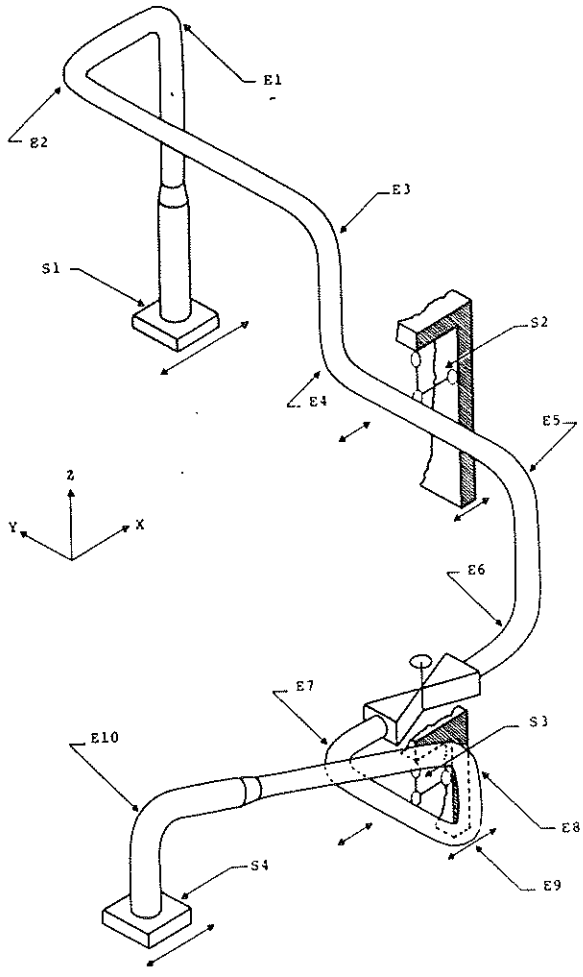

Fig. 1 Test Piping System

A total of four servo-hydraulic actuators (11,000-lb capacity each) were used to provide phase-coherent input motions at the uniaxial shake tables identified in Figure 1 as S1 through S4. The shake tables, or sleds, at S1 and S4 were designed and constructed to resist the large loads and moments introduced by the test piping in five degrees of freedom--permitting only X-direction translational input motions. The two sleds, noted as S2 and S3, were designed and constructed to represent typical piping restraint attachment locations, such as a wall and ceiling. They too permitted input motion in the X direction only; however, the test piping dead weight was taken by rigid hangers with spherical bearings in the vertical direction, permitting relative motions between the test piping and the sleds at S2 and S3 in two directions and rotations about three axes. The different piping restraint devices discussed herein were placed at S2 and S3 and are represented in Figure 1 as the horizontal elements shown at those locations. During these tests, the piping was water filled and pressurized to 1,150 psig.

In total, four tests were run with three different restraint devices installed horizontally at S2 and S3. The first, or baseline, device consisted of rigid struts ($k \simeq 1.1 \times 10^6$ lb/in.) with spherical bearing ends. The overall length of this strut was about 28 inches, the same length as the mechanical piping snubber. The second test case substituted PSA-3 mechanical snubbers for the rigid links at S2 and S3. During the third test case, single visco-elastic GERB RRD-125 damping elements were installed at S2 and S3; and, finally, dual visco-elastic elements were installed at S2 and S3 for the fourth test case.

Photographs of the different restraint devices installed on Sled S2 are shown in Figures 2 through 5.

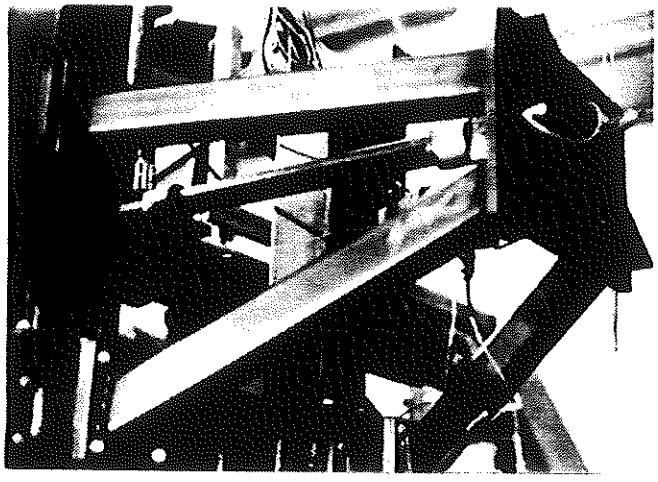

Fig. 2 Rigid Strut Installed at S2

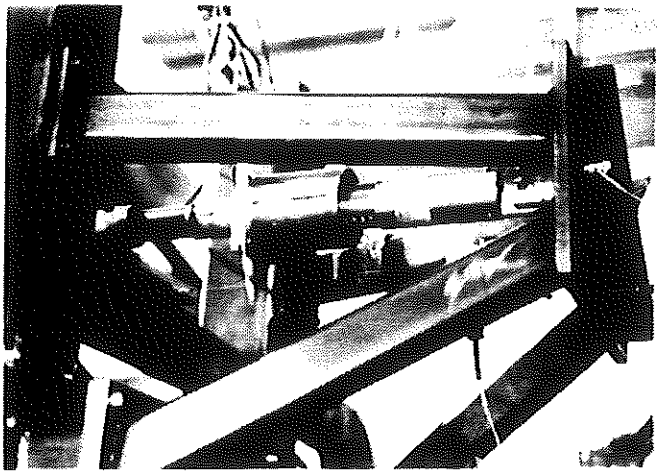

Fig. 3 Mechanical Snubber Installed at S2

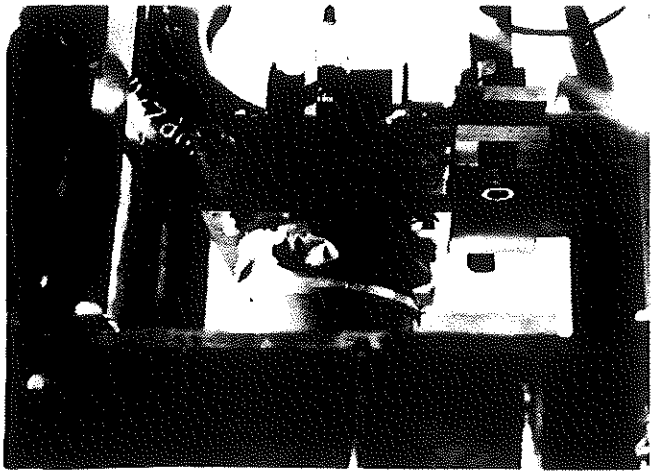

Fig. 4 Visco-Elastic Damper Installed at S2

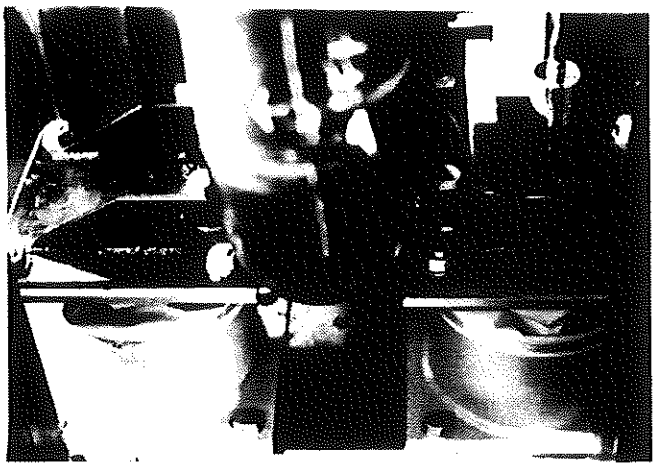

Fig. 5 Double Visco-Elastic Damper Installed at S2

A review of the literature (Refs. 2, 3) indicates a variety of mathematical descriptions for rigid struts and for mechanical snubbers. In general, these idealizations allow for gaps and employ a spring and dashpot in parallel--a Voigt (Kelvin) element. The visco-elastic damping (VED) elements, however, are unique and are best described as a spring and dashpot in series--a Maxwell element. Pseudo-stiffness (k) and damping coefficient (c) curves are available for each VED element size. Figure 6 characterizes the elements used during Test Cases 3 and 4. Pseudo-stiffness increases from zero to a finite value governed by the overall mechanism stiffness as frequency increases; correspondingly, the damping coefficient decreases as a function of frequency. Both stiffness and damping are somewhat greater vertically than in the horizontal plane. The VED is capable of restraining all six degrees of freedom; however, rotational stiffnesses and dampings are significantly less than their translational counter- parts.

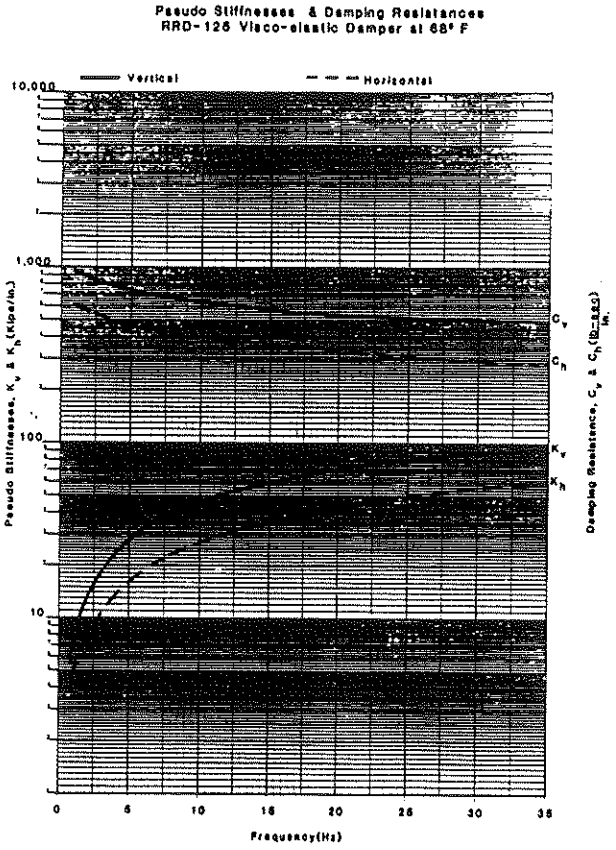

Fig. 6 (k) and (c) Curves for RRD-125 Damper

For each test case, identical synthesized earthquake time histories were input at S1 through S4. Typical acceleration and displacement time histories are shown in Figures 7 and 8, with the corresponding 4-percent damped response spectrum illustrated in Figure 9.

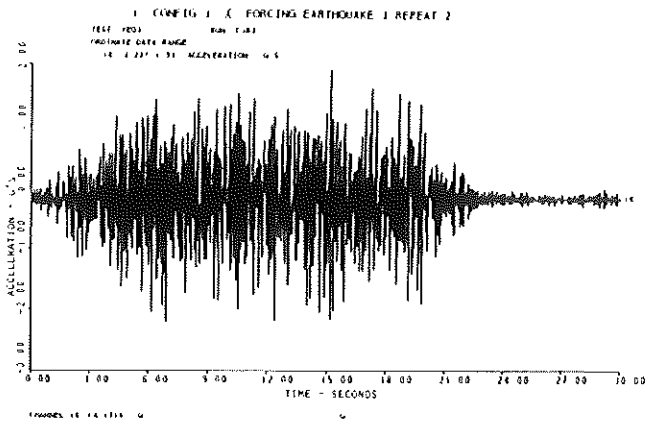

Fig. 7 Typical Input Acceleration Time History

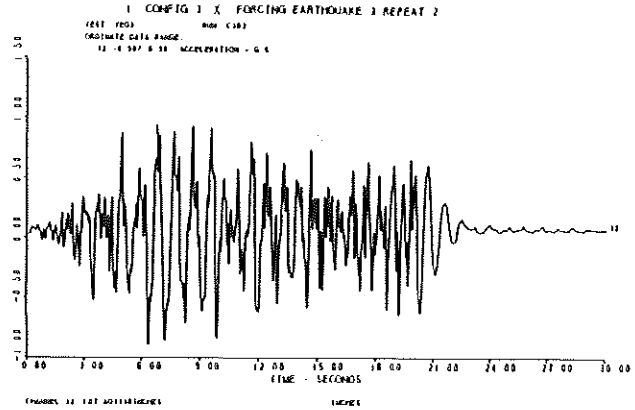

Fig. 8 Typical Input Displacement Time History

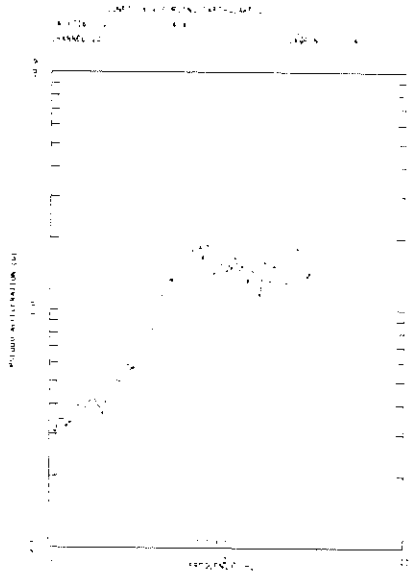

Fig. 9 Typical 4% Damped Test Response Spectra

Peak input acceleration amplitudes varied only four percent over the entire test sequence. The frequency content of the input motion was such that significant fractions of energy were at predicted modes of response. During these tests, input amplitude was limited to a value that would result in peak ASME-allowable Level D stress ratios of 0.5 or less. As a result of this limit, the servo-hydraulic drive system was used at far less than its capacity.

Prior to testing, finite element analysis was used to determine locations on the piping where response and computed stresses would be maximums. Based on the analysis, a total of 64 channels of information were selected to monitor and record input and response values. These 64 channels consisted of 10 accelerometers sensing input motion at the sleds (S1 through S4), 12 accelerometers sensing response of the piping system, 2 displacement transducers sensing input motions, 2 displacement transducers sensing displacement across the restraint device, 6 displacement transducers sensing piping response, 27 strain gages (9 each at the three highest stressed elbows), 1 pressure transducer and 4 load cells to sense restraint loads (where possible). The measurement points (used for this comparison) are pictured in Figure 10. All data channels are summarized in Table 1.

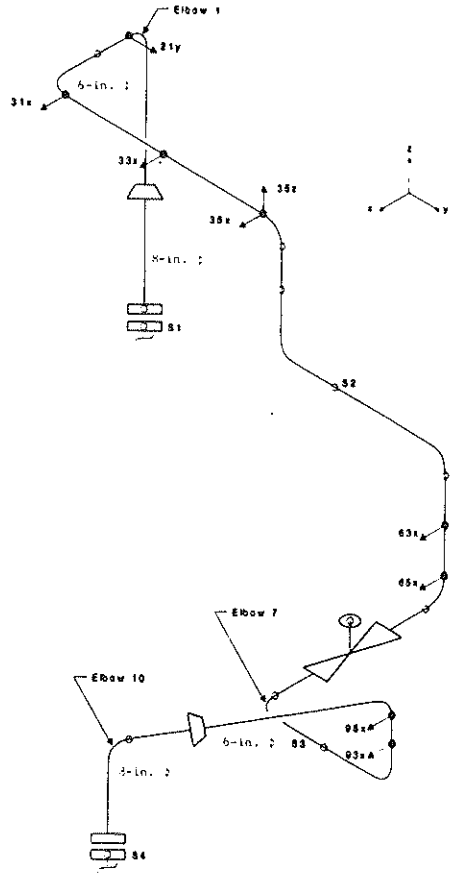

Fig. 10 Data Measurement Points Used in This Paper

TABLE 1: SUMMARY OF ALL DATA CHANNELS

Channel No.(s)	Measured	Location	Direction(s)
1	Resp. Accelera.	21	Y
2	Resp. Accelera.	31	X
3 & 4	Resp. Accelera.	35	X & Y
5	Resp. Accelera.	41	Y
6	Resp. Accelera.	61	X
7	Resp. Accelera.	65	X
8	Resp. Accelera.	71	Z
9	Resp. Accelera.	73	X
10 & 11	Resp. Accelera.	75	Y & Z
12	Resp. Accelera.	95	X
13 thru 15	Input Accelera.	S1	X, Y, & Z
16 & 17	Input Accelera.	S2	X & Y
18 & 19	Input Accelera.	S3	X & Y
20 thru 22	Input Accelera.	S4	X, Y, & Z
23	Input Displace.	S1	X
24	Resp. Displace.	31	X
25	Resp. Displace.	33	X
26	Resp. Displace.	35	X
27	Resp. Displace.	S2	X
28	Resp. Displace.	63	X
29	Resp. Displace.	65	X
30	Resp. Displace.	S3	X
31	Resp. Displace.	93	X
32	Input Displace.	S4	X
33 thru 41	Strains	Elbow 1	
42 thru 50	Strains	Elbow 7	
51 thru 59	Strains	Elbow 10	
60	Load	S2	Z
61	Load	S2	X
63	Load	S3	Z
64	Load	S3	X

Data were collected and analyzed digitally using ANCO's computerized vibration testing and analysis system (CVTAS). Data were presented in several ways. Peak positive and negative values of acceleration, displacement, strain, computed moment, and fraction of allowable stress were printed along with their corresponding time of occurrence immediately following each test case. Plots of the modulus of the Fourier transforms of selected data channels and test response spectra were made from digital tape records of the events. A typical FFT is illustrated in Figure 11. Modal damping was estimated by the half-power bandwidth method as shown in the figure. Review of this data forms the basis of the work presented here. It must be noted that current research indicates (Ref. 4) that the values of half-power damping reported in the data may be distorted; however, since the response waveform did not vary appreciably from one test case to another, the relative values of half-power damping may be compared.

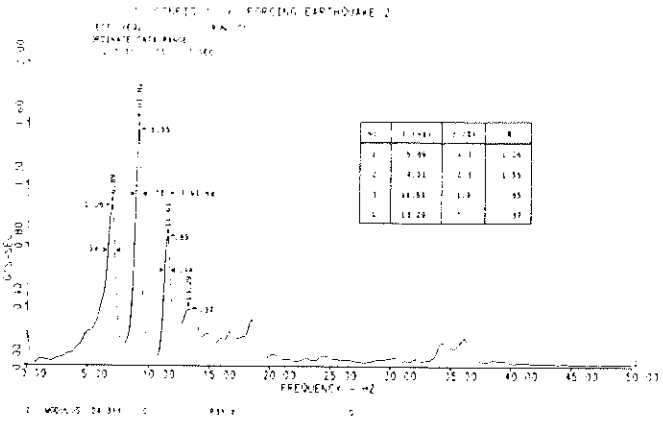

Fig. 11 Typical Fourier Transform of Piping Acceleration Response

EXPERIMENTAL RESULTS

Table 2 presents a summary of piping response for the lowest four modes of vibration with the different restraint devices at S2 and S3. Estimates of the individual resonant frequencies and damping ratios varied somewhat from measurement location to measurement location and are presented as the mean calculated values and their standard deviations. Response amplitudes, defined as the average normalized amplitude of the modulus of the Fourier transform (arbitrary scale) for the lowest four modes of vibration, give an indication of relative modal response amplitudes over the length of the test piping for the different restraint devices. No significant differences in apparent piping stiffness are noted in all but the last test case. The differences in relative damping values and averaged response amplitudes can be seen from one test case to another. In some cases, modal damping could not be estimated from the data because the mode was so highly damped.

TABLE 2: AVERAGED PIPING RESPONSE PARAMETERS WITH DIFFERENT RESTRAINTS AT S2 AND S3

	Mode 1		
Type[1]	$\bar{f}_1$[2] (Hz)	$\bar{\beta}_1$[3] (%)	$\bar{R}_1$[4]
RS	6.88±.1	4.1±.2	.81
MECH	6.75±.06	5.2±.2	.66
1 VED	6.68±.03	6.5±.2	.64
2 VEDs	8.05±.06	7.0±.5	.42

	Mode 2		
Type	$\bar{f}_2$ (Hz)	$\bar{\beta}_2$ (%)	$\bar{R}_2$
RS	9.07±.09	2.4±.1	.76
MECH	9.03±.05	2.6±.1	.63
1 VED	10.36±.17	4.1±1.5	.24
2 VEDs	10.75±.38	4.7±1.1	.20

	Mode 3		
Type	$\bar{f}_3$ (Hz)	$\bar{\beta}_3$ (%)	$\bar{R}_3$
RS	11.41±.14	2.0±.2	.46
MECH	11.35±.09	2.5±.3	.35
1 VED	12.85±.34	5.2±.4	.18
2 VEDs	12.4		.20

	Mode 4		
Type	$\bar{f}_4$ (Hz)	$\bar{\beta}_4$ (%)	$\bar{R}_4$
RS	13.46±.1	3.8±.3	.35
MECH	13.48±.3	2.5±.4	.20
1 VED	14.44±.1	4.1	.23
2 VEDs	15.04±.6		.25

(1) RS = Rigid links at S2 and S3.
MECH = PSA mechanical snubbers at S2 and S3.
1 VED = One GERB RRD-125 VED at S2 and S3.
2 VEDs = Two GERB RRD-125 VEDs at S2 and S3.

(2) $\bar{f}$ = Mean frequency determined at P21y, 31x, 35x, 35z, and 95x and its standard deviation.

(3) $\bar{\beta}$ = Mean half-power damping determined at P21y, 31x, 35x, 35z, and 95x and its standard deviation. Note that these damping values are presented for comparative purposes only and should not be interpreted as actual modal damping ratios.

(4) $\bar{R}$ = Average normalized amplitude of the modulus of the Fourier transform at these locations (i.e., P21y, 31x, 35x, 35z, and 95x).

Peak and averaged values of net peak-to-peak displacements measured during the four test cases are given in Table 3. No significant differences in these values were noted, with the exception of the fourth test case, which incorporated two VEDs at Locations S2 and S3. This arrangement of piping dampers restrained rotation of the pipe about its axis, which stiffened the system and modified the response mode.

TABLE 3: SUMMARY OF PEAK AND AVERAGE* NET DOUBLE AMPLITUDE DISPLACEMENTS WITH VARIOUS RESTRAINTS AT S2 AND S3

Restraint	Peak (in.)	Average (in.)
RS	0.563	0.283
MECH	0.415	0.220
1 VED	0.593	0.260
2 VEDs	0.330	0.160

* Averaged values at Measurement Points P31x, 33x, 35x, 63x, 65x, and 93x.

A summary of peak computed bending moments, torsional moments, and fractions of ASME Level D (1981) stress ratios at the three most highly stressed locations on the test piping is shown in Table 4. Significant variation in these computed values can be seen. Table 5 summarizes the peak values of allowable stress ratios and averages them over the length of the test piping system.

TABLE 4: SUMMARY OF PEAK BENDING MOMENTS, TORSION, AND COMPUTED 1981 STRESS RATIO* AT SELECTED ELBOWS WITH VARIOUS RESTRAINTS AT S2 AND S3 (M_y, M_z, and T in units of in.-kips)

Type	M_y	M_z	T	$\bar{M}$	R
Elbow 1 (6-in. ϕ)					
RS	39.7	32.0	25.3	56.9	.487
MECH	24.0	20.0	21.5	37.9	.325
1 VED	29.3	15.1	13.8	35.7	.306
2 VEDs	18.8	11.4	15.0	26.6	.228
Elbow 7 (6-in. ϕ)					
RS	38.5	23.4	31.0	54.7	.468
MECH	36.3	14.5	32.5	50.8	.435
1 VED	43.1	12.3	22.9	50.3	.431
2 VEDs	34.8	10.8	21.0	42.1	.360
Elbow 10 (8-in. ϕ)					
RS	50.0	54.2	68.0	100.3	.467
MECH	36.6	47.5	66.1	89.2	.415
1 VED	34.1	32.9	57.6	74.6	.347
2 VEDs	34.7	30.5	55.7	72.4	.337

TABLE 5: COMPARISON OF 1981 ASME LEVEL D STRESS RATIOS* DURING SIMULATED EARTHQUAKE EXCITATION

S2 and S3 Horizontal Restraint	Stress Ratios (R)			
	Elbow 1	Elbow 7	Elbow 10	Average
Rigid	.487	.468	.467	.474
Mechanical Snubber	.325	.435	.415	.392
Single VED	.306	.431	.347	.361
Double VEDs	.228	.360	.337	.308

$$* \; R = \frac{B_1 \frac{PD_o}{2t} + B_2 \frac{\bar{M}}{Z}}{3.0 \, S_h} \; ; \quad \bar{M} = \sqrt{M_x^2 + M_y^2 + M_z^2}$$

B_1 and B_2 in accord with 1981 Winter Addenda rules;

where R = fraction of allowable stress limit and

S_h = 15,000 psi.

CONCLUSIONS

It has been demonstrated that differences in piping response can be due to the method of piping restraint at levels of input relevant to seismic events.

An alternative piping restraint has been discussed (VED)* that significantly reduces the dynamic response of piping during earthquake excitation. This rather simple device has no moving parts, does not lock up, has no deadband, and will restrain six degrees of freedom. It functions by placing a very viscous liquid in shear between the piping and the support. Since it does not lock up, thermal expansion occurs freely; and in addition, inertial loads on supports may be reduced. The device appears to be inherently maintenance free.

The test results presented herein demonstrate that a single VED piping damper can provide the equivalent restraint of a mechanical snubber. The peak piping stresses at critical locations resulting from simulated earthquake support motion are comparable for a test piping system restrained by either a mechanical snubber or a VED. In addition, the VED concept allows simple placement of an additional VED that can provide a moment restraint in addition to a uniaxial restraint. Thus, dual VEDs can reduce stresses at critical locations by providing additional dynamic stiffness, yet allowing unrestrained thermal expansion.

* Manufactured by GERB, gmbh, Berlin, FRG.

REFERENCES

1. ASME Boiler and Pressure Vessel Code, Section III, Division I, Subsection NC (Class 2 Components), 1980 edition.

2. Reddy, D.P., and Agbabian, M.S., "Nonlinear Models for Mechanical Seismic Snubbers," ASME Paper 82-WA/PVP-3, presented at the 1982 ASME Winter Meeting, Phoenix, Arizona, November 1982.

3. Severud, L.K., and Summers, G.D., "Design Considerations for Mechanical Snubbers," PVP-42, "Component Support Snubbers - Design, Application, and Testing," presented at the ASME Pressure Vessels and Piping Conference, San Francisco, California, August 1980.

4. Chitty, D.E., et al., "Damping in Nonlinear Piping Systems," ASME Paper 82-WA/PVP-10, presented at the ASME Winter Meeting, Phoenix, Arizona, November 1982.